Three-Time-Point PET Analysis of ^{68}Ga-FAPI-46 in a Variety of Cancers

Mahnoosh Naeimi[1], Peter L. Choyke[2], Katharina Dendl[1], Yuriko Mori[3], Fabian Staudinger[1], Tadashi Watabe[4], Stefan A. Koerber[5], Manuel Röhrich[1], Jürgen Debus[5], Clemens Kratochwil[1], Uwe Haberkorn[1], and Frederik L. Giesel[1,3,6]

[1]Department of Nuclear Medicine, University Hospital Heidelberg, Heidelberg, Germany; [2]Molecular Imaging Branch, Center for Cancer Research, National Cancer Institute, National Institutes of Health, Bethesda, Maryland; [3]Department of Nuclear Medicine, Medical Faculty of Heinrich Heine University, University Hospital Düsseldorf, Düsseldorf, Germany; [4]Department of Nuclear Medicine and Tracer Kinetics, Osaka University Graduate School of Medicine, Osaka, Japan; [5]Department of Radiation Oncology, University Hospital Heidelberg, Heidelberg, Germany; and [6]Institute of Radiation Science, Osaka University, Osaka, Japan

See an invited perspective on this article on page 623.

A growing family of ^{68}Ga-fibroblast activation protein inhibitor (FAPI) PET probes has shown promise in imaging a variety of medical conditions. ^{68}Ga-FAPI-46, in particular, has emerged as unique for both its diagnostic and its theranostic applications; however, the optimal timing of PET remains unclear. Therefore, we evaluated uptake at 3 time points after ^{68}Ga-FAPI-46 administration in a spectrum of tumor types. **Methods:** The cohort consisted of 43 patients with diverse cancer diagnoses undergoing ^{68}Ga-FAPI-46 PET/CT at 3 time points (10 min, 1 h, and 3 h). We determined the tracer uptake based on SUV_{mean} and SUV_{max} and on tumor-to-background-ratios (TBRs) (SUV_{max}/SUV_{mean}). **Results:** There were 171 lesions in the 43 patients. Comparing all lesions at different time points, the mean SUV_{max} was maximal at 10 min (8.2) and declined slightly at 1 h (8.15) and 3 h (7.6) after tracer administration. Similarly, the mean SUV_{max} log still had a similar pattern in primary lesions at 10 min, 1 h, and 3 h ($n = 30$; 0.98, 1.01, and 0.98, respectively), lymph node metastases ($n = 37$; 0.82, 0.84, and 0.81, respectively), and distant metastases ($n = 104$; 0.81, 0.79, and 0.74, respectively). TBR also showed nonsignificant differences at the 3 times. **Conclusion:** ^{68}Ga-FAPI-46 PET/CT imaging revealed remarkably stable tumor and background uptake as determined by SUV metrics and maintained high TBRs within 3 h of injection. Thus, it may be possible to scan with ^{68}Ga-FAPI-46 within 10–20 min of injection, improving workflow and decreasing patient wait times. Confirmation of these findings in a larger cohort is under way.

Key Words: FAPI; fibroblast activation protein; PET; PET/CT; 3-time-point

J Nucl Med 2023; 64:618–622
DOI: 10.2967/jnumed.122.264941

Reliable staging tools are vital for oncologic management. Molecular imaging probes have been advancing rapidly and are capable of detecting cancer with high sensitivity. Fibroblast activation protein (FAP) is expressed by cancer-associated fibroblasts in many cancer types and is implicated in tumor cell migration, invasion, cell

Received Sep. 20, 2022; revision accepted Oct. 4, 2022.
For correspondence or reprints, contact Frederik L. Giesel (frederik.giesel@med.uni-duesseldorf.de).
Published online Nov. 10, 2022.

TABLE 1
Various Tumor Entities in 43 Patients

Tumor type	Patients (*n*)
Sarcoma	2
Anal cancer	4
Colorectal cancer	6
Lung cancer	11
Pancreatic cancer	5
Esophageal cancer	2
Head and neck cancer	3
Adrenocortical carcinoma	3
Breast cancer	2
Ovarian cancer	1
Bladder cancer	1
Lymphoma	1
Prostate cancer	1
Neuroblastoma	1

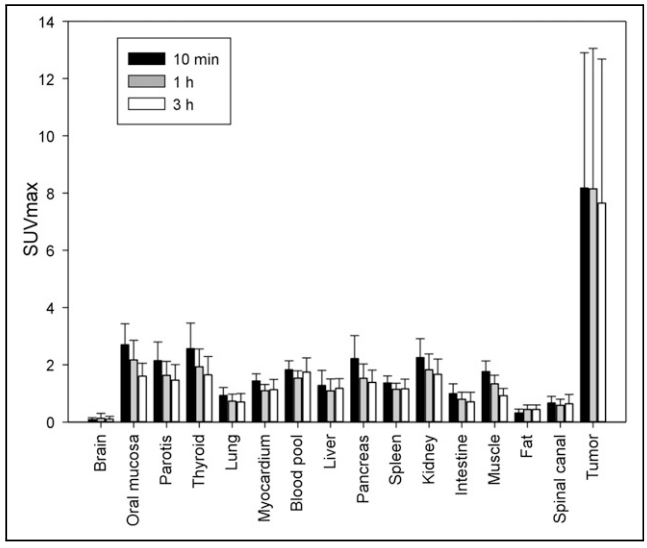

FIGURE 1. Biodistribution SUV_{max} of ^{68}Ga-FAPI-46 PET at 3 time points in normal organs vs. all tumor lesions.

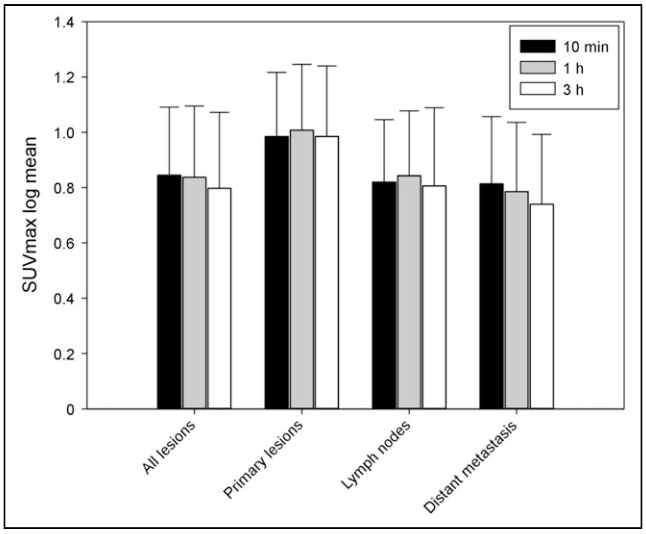

FIGURE 2. Tumor uptake (SUV_{max} log) through time points (10 min, 1 h, and 3 h) in all lesions ($n = 171$), primary lesions ($n = 30$), lymph node metastases ($n = 37$), and distant metastases ($n = 104$).

signaling, and tumor angiogenesis (*1–3*). FAP therefore represents an interesting target for new molecular imaging and therapeutic agents. The development of a quinoline-based FAP inhibitor (FAPI) with high affinity for FAP represents an opportunity to exploit this target for PET imaging (*4*). Such radiolabeled quinoline-based ligands have shown promising results in previous studies (*5–7*).

By convention, most molecular imaging agents are scanned 1 h after injection. Likewise, for FAP imaging, most of the previously published studies involved acquiring static PET images 1 h after injection (*7*). However, there are conflicting reports in the literature about optimal incubation times for FAPI agents, and no conclusive data have been published (*8–12*). In this investigation, we compared different incubation times of the agent ^{68}Ga-FAPI-46 in different cancers at 3 time points: 10 min, 1 h, and 3 h.

MATERIALS AND METHODS

Patient Cohort

This was a retrospective study of 43 patients with various malignancies who underwent ^{68}Ga-FAPI-46 PET/CT. The tumor types are summarized in Table 1. All imaging was performed at a single center, and all patients were referred by their attending oncologist or radiation oncologist for 1 of 3 reasons: to improve delineation of the target volume for radiotherapy planning, to restage because of ambiguous findings on conventional imaging, or to follow up. All patients gave written informed consent to undergo ^{68}Ga-FAPI PET/CT on an individual-patient basis following national regulations and the declaration of Helsinki. The radiopharmaceutical was synthesized and labeled according to the German Pharmaceutical Act, §13(2b). The data were analyzed retrospectively with the approval of the local ethics committee (S016/2018).

Radiopharmaceuticals and ^{68}Ga-FAP-46 PET/CT Imaging

^{68}Ga-FAPI-46 was synthesized and labeled as previously described (*13*). A non–contrast-enhanced low-dose CT scan (130 keV, 30 mAs, CareDose; reconstructed with a soft-tissue kernel to a slice thickness of 5 mm) and a Biograph mCT Flow scanner (Siemens) were used for imaging. All PET scans were acquired in 3-dimensional mode (matrix, 200 × 200). Each patient underwent PET/CT imaging at 3 time points after radiotracer injection: 10 min, 1 h, and 3 h. Patients were evaluated for adverse effects at several times during the examination, and vital signs were monitored until 30 min after the end of the examination.

Image Evaluation

Tracer uptake and biodistribution were quantified by SUV_{max} and SUV_{mean} at 10 min, 1 h, and 3 h after injection of ^{68}Ga-FAPI-46 (Fig. 1). For SUV calculation, e.soft software (Siemens) was used to manually draw circular volumes of interest around tumor lesions on transaxial slices at 1 h and were automatically transferred to the images obtained at 10 min and 3 h, using a 3-dimensional volume of interest at a 60% isocontour. Normal organs were evaluated with a 1-cm-diameter (for small organs: thyroid, parotid gland, myocardium, oral mucosa, spinal cord, and ovary) or 2-cm-diameter (brain, muscle, liver, pancreas, spleen, kidney, fat, aortic lumen content, lung, mammary gland, and endometrium) spheric region of interest (ROI) placed completely inside the organ parenchyma. For quantification of image contrast, tumor-to-background ratios (TBRs) were calculated. The formula was calculated using the geometric mean of the quotients of lesion tissue (SUV_{max}) to background tissue (SUV_{mean}). Liver tissue, oral mucosa, fat, and gluteal muscle were chosen as background tissue. The ^{68}Ga-FAPI PET/CT scans were analyzed in consensus by a board-certified radiologist, a board-certified radiation oncologist, and 2 board-certified nuclear medicine physicians.

Statistics

Descriptive analyses of patients and their tumors were performed. We determined SUVs using the median, arithmetic mean, SD and logarithm of SUVs to minimize potential mistakes during arithmetic mean calculations. The SUVs and SUV logs were distributed normally; therefore, a 2-sided *t* test with paired samples was used to compare ^{68}Ga-FAPI-46 SUVs in primary cancer, lymph node metastases, and distant metastases at the 3 time points. A *P* value of less than 0.05 was defined

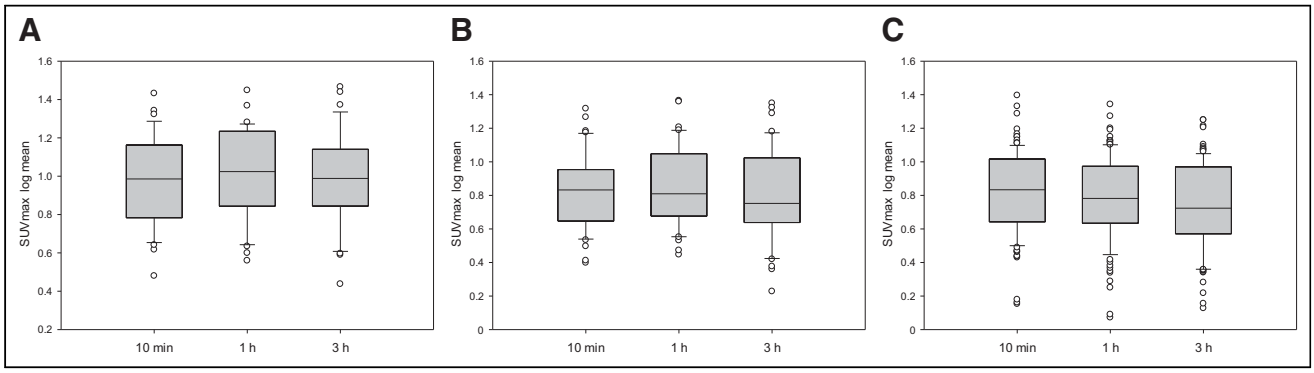

FIGURE 3. Box plot of ^{68}Ga-FAPI-46 PET distribution through time points (10 min, 1 h, and 3 h), with uptake (SUV_{max} log) by primary lesions (A), lymph node metastases (B), and distant metastases (C).

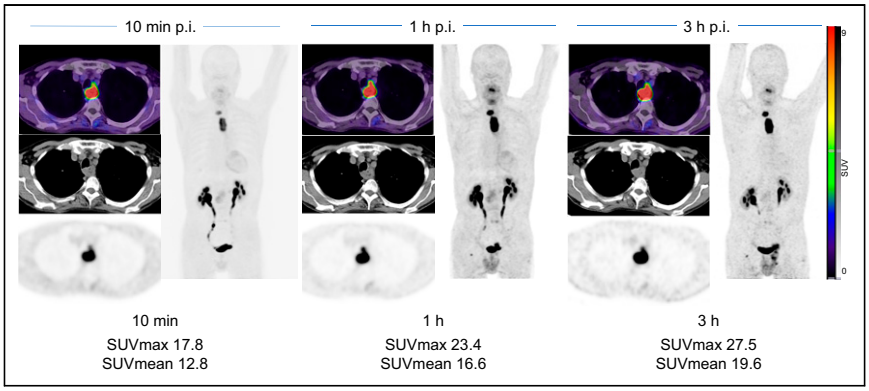

FIGURE 4. Case example of 63-y-old patient with esophageal cancer. ^{68}Ga-FAPI-46 PET/CT was performed for irradiation planning before definitive radiochemotherapy. ^{68}Ga-FAPI-46 PET was performed (10 min, 1 h, and 3 h) after injection (p.i.).

as statistically significant. All statistical analyses were performed using Excel (version 16.16; Microsoft) for Mac (Apple).

RESULTS

Study Population

Our data consisted of 43 patients with various malignancies, who are summarized in Table 1. Lesions consisted of primary cancers or tumor relapse ($n = 30$), lymphatic metastases ($n = 37$), and distant metastases ($n = 104$). The following tumor entities were included: lung cancer ($n = 11$); colorectal cancer ($n = 6$); pancreatic cancer ($n = 5$); anal cancer ($n = 4$); adrenocortical carcinoma ($n = 3$); head and neck cancer ($n = 3$); sarcoma, breast cancer, and ovarian cancer ($n = 2$); and bladder cancer, neuroblastoma, lymphoma, and prostate cancer ($n = 1$) (Table 1).

Biodistribution in Normal Organs

The biodistribution of ^{68}Ga-FAPI-46 in normal organs is shown in Figure 1, with stable low background activity; a mean SUV_{max} of 1.6, 1.3, and 1.2, at 10 min, 1 h, and 3 h, respectively; and a mean SUV_{mean} of 1.2, 1.0, 0.9, at 10 min, 1 h, and 3 h, respectively.

Biodistribution in normal organs decreased slightly from the 10-min to 3-h time points; however, no significant difference in SUV_{max} was observed among all normal organs (10 min vs. 3 h; $P = 5.5$, $n = 806$). The highest uptake in normal organs was always obtained on the first (10 min) scan, except for fat tissue. The overall highest uptake was in the oral mucosa and thyroid tissue. Thus, within the oral mucosa, the mean SUV_{max} at 10 min, 1 h, and 3 h was 2.7, 2.2, and 1.6, respectively, whereas for thyroid tissue it was 2.6, 1.9, and 1.6, respectively. The lowest tracer uptake was in the brain, where mean SUV_{max} was 0.1, 0.1, and 0.1, respectively (Fig. 1).

Tumor Uptake

There were 171 lesions detected. All lesions were detected at all time points. At 10 min, 1 h, and 3 h, the mean SUV_{max} log was 0.98, 1.0, and 0.98, respectively, for primary lesions and local relapse ($n = 30$); 0.82, 0.84, and 0.80, respectively, for lymph node metastases ($n = 37$); and 0.81, 0.78, and 0.74, respectively, for distant metastases ($n = 104$). No significant difference was seen. The analysis of primary lesions or local relapse showed no significant difference in SUV_{max} at the 3 time points in 2-way comparisons (10 min vs. 1 h, $P = 0.2$; 10 min vs. 3 h, $P = 0.98$; and 1 h vs. 3 h, $P = 0.2$). The analysis of lymph node metastases ($n = 37$) showed increased tumor uptake at 1 h compared with the other 2 time points, with a significant difference for the comparison between 1 and 3 h ($P = 0.02$). There were no significant differences in SUV_{max} at other time points (10 min vs. 1 h, $P = 0.26$; 10 min vs. 3 h, $P = 0.66$). The analysis of distant metastases showed a significant decrease in tumor uptake through the time points. The highest tumor uptake was observed at 10 min (10 min vs. 1 h, $P = 0.02$; 10 min vs. 3 h, $P = 3.05E^{-5}$; 1 h vs. 3 h, $P = 1.27E^{-5}$) (Figs. 2 and 3). Two examples of patients with tumors with similar uptake on ^{68}Ga-FAPI-46 scans at the 3 time points are shown in Figures 4 and 5.

TBRs

Most background tissues showed a decrease in SUV_{max} and SUV_{mean} at longer incubation times, with the exception of fat tissue, which, at 10 min, 1 h, and 3 h, had a low SUV_{max} of 0.32, 0.44, and 0.44, respectively, and brain parenchyma, with an SUV_{max} of 0.09, 0.13, and 0.1, respectively. As expected, the primary and local relapse lesions demonstrated excellent contrast with normal tissue, and this contrast increased through the time points except for TBR versus fat tissue. Increased TBR could also be measured in lymph nodes and distant metastases except for tumor-to-fat ratios, which slightly decreased (Fig. 6). High TBRs were seen in primary and local relapse lesions versus fat tissue even after 3 h.

Quantifying ^{68}Ga-FAPI-46 Uptake in Different Types of Tumors

The highest average SUV_{max} (>20) in ^{68}Ga-FAPI-46 scans was in primary lesions. The highest SUV_{max} was in esophageal cancer (27.5; 3 h) and primary bladder cancer (29.2; 3 h). The highest SUV_{max} among all lymph node metastases was in esophageal lymph node metastases (19.5; 3 h). Among the distant metastases, breast cancer metastases demonstrated the highest SUV_{max} (15.7; 10 min) (Fig. 7).

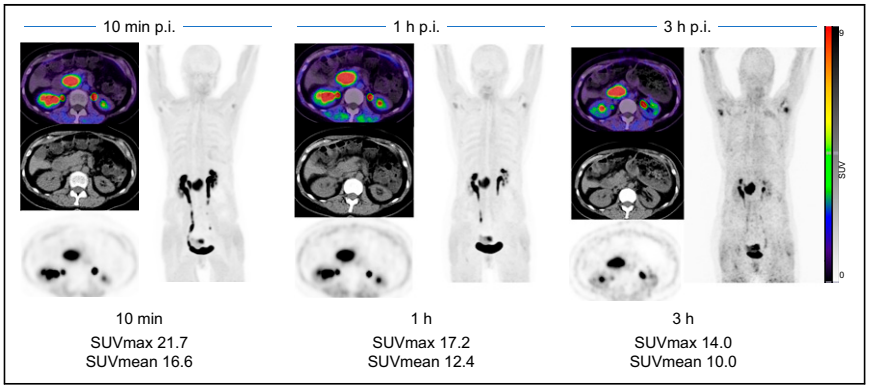

FIGURE 5. Case example of 60-y-old patient with pancreatic cancer. ^{68}Ga-FAPI-46 PET/CT was performed because of suspected recurrent mass in pancreatic head on ultrasound. ^{68}Ga-FAPI-46 PET was performed (10 min, 1 h, and 3 h) after injection (p.i.).

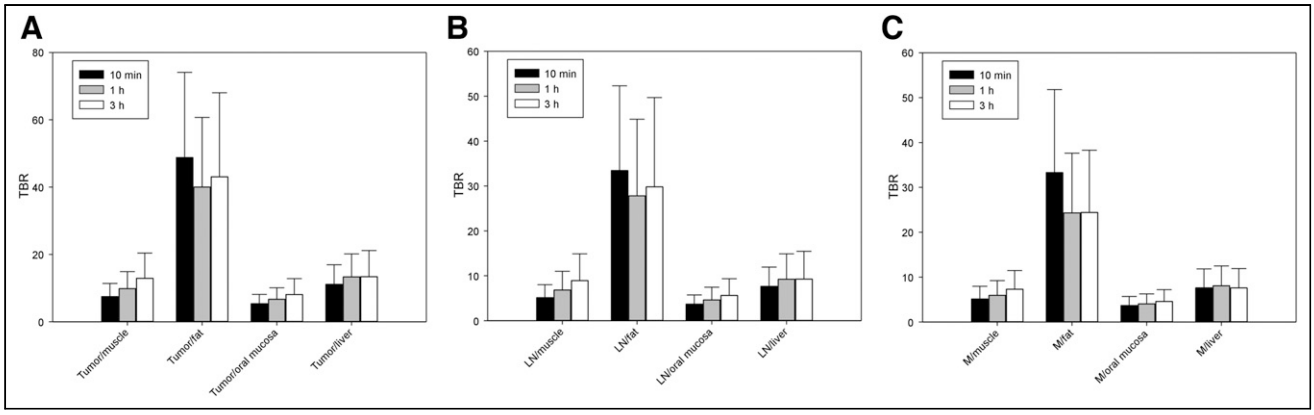

FIGURE 6. TBR through time points (10 min, 1 h, and 3 h) for tumor (primary/release; $n = 30$) (A), lymph node metastases ($n = 37$) (B), and distant metastases ($n = 104$) (C). LN = lymph node; M = distant metastases.

DISCUSSION

The aim of this study was to evaluate the optimal uptake time for ^{68}Ga-FAPI-46 based on time points between 10 min and 3 h after injection. The SUV_{max} for ^{68}Ga-FAPI-46 was remarkably stable at all 3 time points, although the 10-min time point generally had a slightly higher SUV_{max}. The detection rate of tumors was equal at all time points, implying that a diagnostic study can be achieved by 10 min after injection, which will have implications for patient throughput and decreased patient waiting times in the nuclear medicine department. Our study had findings similar to a previous analysis of ^{68}Ga-FAPI PET acquisitions at 5 time points earlier than 60 min regarding the best time for diagnostic imaging (*14*). However, because of the similar detection rate between 10 min and 1 h after injection and a slightly higher tumor uptake at the 10 min time point, we recommend 10–20 min after injection as the best time point for diagnostic imaging acquisition instead of 30–40 min after injection (*14*).

The steady uptake of ^{68}Ga-FAPI-46 also has implications for its use as a targeted theranostic agent for which high dose delivery will be achieved early and will be maintained over at least several hours (*15*). Meanwhile, background uptake, largely responsible for toxicity in targeted treatments, appears to clear rapidly over 3 h, resulting in high TBRs consistent with prior reports (*4,13*).

^{68}Ga-FAPI-46 is one of many FAPI derivatives but appears to have several desirable features, including high affinity for the target and biologic stability (*13,16*). ^{68}Ga-FAPI-46 showed no significant washout between 10 min and 3 h, in comparison to other FAPI derivatives such as FAPI-02 and FAPI-04, which in a previous study showed 75% and 25% washout at 3 h after injection, respectively (*17*), making ^{68}Ga-FAPI-46 more valuable. Although that study (*17*) had a limited patient cohort, all 3 FAPI derivatives showed similar biodistributions und high TBRs between 10 min and 3 h.

^{68}Ga-FAPI-46 uptake was compared in primary lesions, lymph node metastases, and distant metastases in a spectrum of cancer types. The SUV_{max} log decreased over time in all stages of disease, and the TBR commensurately increased over the same period because of background washout. The findings were consistent regardless of the stage of the cancer lesion. These findings confirm prior studies showing similar results in a variety of cancers (*8,11,18–20*). It is expected that there will be minor differences in various single-institution studies because of differences in the composition of the patient cohort and types of tumor. Hu et al. found similar results using 2 related derivatives of FAPI: ^{18}F-FAPI-42 and ^{68}Ga-FAPI-04 (*9*).

The TBRs obtained in this study were based on various background tissues including muscle, oral mucosa, and liver. In each case, the TBR increased as expected through time. This finding is in line with similar previous studies (*11,18*). The highest TBR is seen with comparisons of the tumor to fat tissue, resulting in very high values even up to 3 h after injection. The highly favorable TBR obtained with

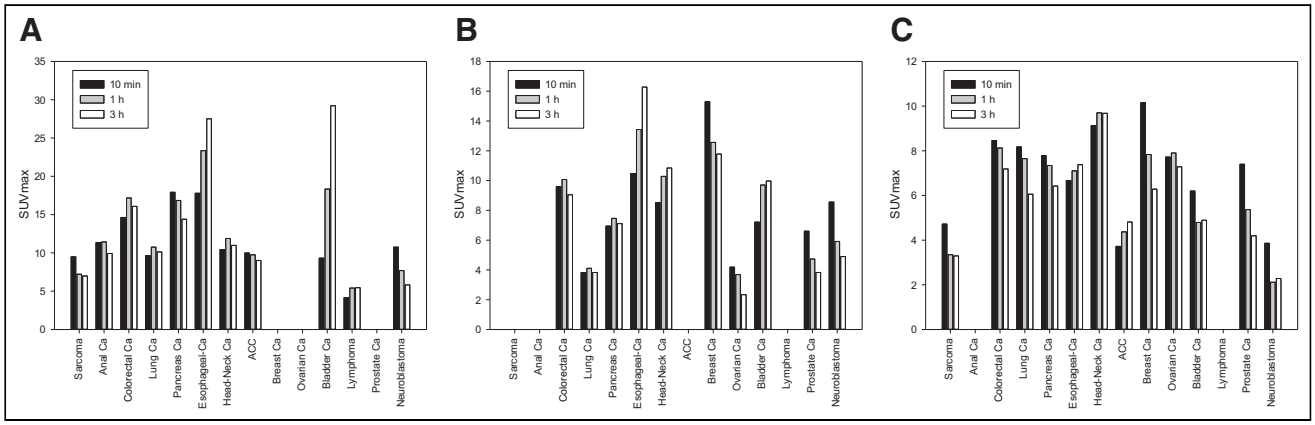

FIGURE 7. ^{68}Ga-FAPI-46 mean SUV_{max} in various tumor entities: primary/relapse tumors ($n = 30$) (A), lymph node metastases ($n = 37$) (B), and distant metastases ($n = 104$) (C). ACC = adrenocortical carcinoma; BC = bronchial carcinoma; CA = cancer; CRC = colorectal cancer; mama = mammary gland.

FAPI agents in general and ^{68}Ga-FAPI-46 specifically stands in contrast to the highly variable TBR obtained with ^{18}F-FDG PET scans.

This study had several limitations. Because of the limited number of patients, no reliable comparisons among tumor types was possible. False-positive findings in nontumorous lesions or inflammation, such as in the pancreas, could have influenced the results since histologic validation was not possible for all lesions. However, all patients were known to have extensive cancer based on conventional imaging, and it is highly likely that most lesions measured in this study were cancers.

CONCLUSION

We found that ^{68}Ga-FAPI-46 is a robust FAPI-targeting molecule that is highly reliable for diagnostic imaging as early as 10 min after injection. This result might have important implications for improving workflow and decreasing wait times in nuclear medicine departments, compared with more traditional PET agents such as ^{18}F-FDG PET. The results also suggest that ^{68}Ga-FAPI-46 might be an excellent theranostic agent, as it binds to its target soon after injection and maintains a high level of uptake over several hours while steadily decreasing background activity.

DISCLOSURE

Uwe Haberkorn, Clemens Kratochwil, and Frederik Giesel have filed a patent application for quinoline-based FAP-targeting agents for imaging and therapy in nuclear medicine and have shares in a consultancy group for iTheranostics. Frederik Giesel is an advisor to ABX, Telix Pharma, Alpha Fusion, and SOFIE Biosciences. No other potential conflict of interest relevant to this article was reported.

ACKNOWLEDGMENT

We highly appreciate the support of Patrick Pätsch for data analysis.

KEY POINTS

QUESTION: What is the tumor residence of ^{68}Ga-FAPI-46 from 10 min to 3 h after injection in various cancers?

PERTINENT FINDINGS: ^{68}Ga-FAPI-46 is characterized by rapid and persistent tumor residence from 10 min to up to 3 h, enabling robust TBRs.

IMPLICATIONS FOR PATIENT CARE: ^{68}Ga-FAPI-46 has rapid uptake in different tumor entities and is retained in the tumor for 3 h after injection, findings that impact imaging procedures and also possible future theranostic applications of FAP ligands.

REFERENCES

1. LeBleu VS, Kalluri R. A peek into cancer-associated fibroblasts: origins, functions and translational impact. *Dis Model Mech.* 2018;11:dmm029447.
2. Kalluri R. The biology and function of fibroblasts in cancer. *Nat Rev Cancer.* 2016;16:582–598.
3. Sahai E, Astsaturov I, Cukierman E, et al. A framework for advancing our understanding of cancer-associated fibroblasts. *Nat Rev Cancer.* 2020;20:174–186.
4. Loktev A, Lindner T, Burger EM, et al. Development of fibroblast activation protein-targeted radiotracers with improved tumor retention. *J Nucl Med.* 2019;60:1421–1429.
5. Koerber SA, Staudinger F, Kratochwil C, et al. The role of ^{68}Ga-FAPI PET/CT for patients with malignancies of the lower gastrointestinal tract: first clinical experience. *J Nucl Med.* 2020;61:1331–1336.
6. Chen H, Pang Y, Wu J, et al. Comparison of [^{68}Ga]Ga-DOTA-FAPI-04 and [^{18}F] FDG PET/CT for the diagnosis of primary and metastatic lesions in patients with various types of cancer. *Eur J Nucl Med Mol Imaging.* 2020;47:1820–1832.
7. Kratochwil C, Flechsig P, Lindner T, et al. ^{68}Ga-FAPI PET/CT: tracer uptake in 28 different kinds of cancer. *J Nucl Med.* 2019;60:801–805.
8. Röhrich M, Leitz D, Glatting FM, et al. Fibroblast activation protein-specific PET/CT imaging in fibrotic interstitial lung diseases and lung cancer: a translational exploratory study. *J Nucl Med.* 2022;63:127–133.
9. Hu K, Wang L, Wu H, et al. [^{18}F]FAPI-42 PET imaging in cancer patients: optimal acquisition time, biodistribution, and comparison with [^{68}Ga]Ga-FAPI-04. *Eur J Nucl Med Mol Imaging.* 2022;49:2833–2843.
10. Wang S, Zhou X, Xu X, et al. Dynamic PET/CT imaging of ^{68}Ga-FAPI-04 in Chinese subjects. *Front Oncol.* 2021;11:651005.
11. Ferdinandus J, Kessler L, Hirmas N, et al. Equivalent tumor detection for early and late FAPI-46 PET acquisition. *Eur J Nucl Med Mol Imaging.* 2021;48:3221–3227.
12. Geist BK, Xing H, Wang J, et al. A methodological investigation of healthy tissue, hepatocellular carcinoma, and other lesions with dynamic ^{68}Ga-FAPI-04 PET/CT imaging. *EJNMMI Phys.* 2021;8:8.
13. Meyer C, Dahlbom M, Lindner T, et al. Radiation dosimetry and biodistribution of ^{68}Ga-FAPI-46 PET imaging in cancer patients. *J Nucl Med.* 2020;61:1171–1177.
14. Glatting FM, Hoppner J, Liew DP, et al. Repetitive early ^{68}Ga-FAPI PET acquisition comparing ^{68}Ga-FAPI-02, ^{68}Ga-FAPI-46, and ^{68}Ga-FAPI-74: methodologic and diagnostic implications for malignant, inflammatory/reactive, and degenerative lesions. *J Nucl Med.* 2022;63:1844–1851.
15. Giesel FL, Kratochwil C, Lindner T, et al. ^{68}Ga-FAPI PET/CT: biodistribution and preliminary dosimetry estimate of 2 DOTA-containing FAP-targeting agents in patients with various cancers. *J Nucl Med.* 2019;60:386–392.
16. Röhrich M, Naumann P, Giesel FL, et al. Impact of ^{68}Ga-FAPI PET/CT imaging on the therapeutic management of primary and recurrent pancreatic ductal adenocarcinomas. *J Nucl Med.* 2021;62:779–786.
17. Giesel FL, Kratochwil C, Schlittenhardt J, et al. Head-to-head intra-individual comparison of biodistribution and tumor uptake of ^{68}Ga-FAPI and ^{18}F-FDG PET/CT in cancer patients. *Eur J Nucl Med Mol Imaging.* 2021;48:4377–4385.
18. Mona CE, Benz MR, Hikmat F, et al. Correlation of ^{68}Ga-FAPi-46 PET biodistribution with FAP expression by immunohistochemistry in patients with solid cancers: interim analysis of a prospective translational exploratory study. *J Nucl Med.* 2022;63:1021–1026.
19. Ferdinandus J, Costa PF, Kessler L, et al. Initial clinical experience with ^{90}Y-FAPI-46 radioligand therapy for advanced-stage solid tumors: a case series of 9 patients. *J Nucl Med.* 2022;63:727–734.
20. Kratochwil C, Giesel FL, Rathke H, et al. [^{153}Sm]samarium-labeled FAPI-46 radioligand therapy in a patient with lung metastases of a sarcoma. *Eur J Nucl Med Mol Imaging.* 2021;48:3011–3013.